Raman-Nath thin gratings of low-saturated dynamic recording materials

S.Bugaychuk[1], E.Korchemskaya[1], N.Burykin[2]

[1]Institute of Physics of the National Academy of Sciences,
46 Prospect Nauki, Kiev 03039, Ukraine, bugaich@iop.kiev.ua,
[2]Institute of Applied Optics of the National Academy of Sciences,
10G Kudryavskaya Str., Kiev 03053, Ukraine.

Received 07.12.2001

Abstract

The holographic kinetics of organic polymer thin films with low-saturated absorption are considered both for self-diffraction and diffraction of a weak probe beam in Raman-Nath conditions. The coupling effect between different diffracted orders is taking into account. The coupling effect results in considerable increase of the diffraction efficiency of self-diffracted beams compared with the diffraction of the probe beam were shown. For the region of deep saturation the maximum diffraction efficiency is higher than in the region far from the saturation. The maximum of diffraction efficiency is reached for considerable shorter time in grating recording kinetics in the region of deep saturation. This opens the perspective of using those materials for novelty filter. The experimental results on low-saturated dry bacteriorhodopsin films well agree the theoretical predictions.

Keywords: low-saturated recording materials, dynamic holography gratings, Raman-Nath conditions, coupling effect of different diffracted orders.

PACS: 42.25Fx

1. Introduction

In shown last decades, thin films on the base of optical materials with nonlinear saturable absorption can be successfully used for the real-time applications such as phase conjugation, image processing, and optical switching [1-3]. The large optical nonlinearities in the materials are those due to saturable absorption with a small value of the saturation intensity. In the materials known as DuPont photopolymers [3] and fluorescein-doped boric acid grass that has a very small saturation intensity of ~15mWcm^{-2} [5], for which two- and four-wave mixing holographic experiments were studied both in the steady state and in kinetics. The materials can be used with high efficiency in the polarization holography [6], as, in particular, it was shown for the layers of methyl orange introduced in a matrix of polyvinyl alcohol [7]. The conventionally used experiments exploit the Bragg-conditions from thick holograms as well as diffraction of probe beams, intensities of which are much smaller than the ones of coupled writing beams. Recently Raman-Nath thin gratings in self-diffraction conditions on low-saturated bacteriorhodopsin films promise much for real time analysis of object motion [8, 9].

In the present paper we develop the modeling for comparable kinetics of self-diffraction of recording beams and the

diffraction of a weak probe beam in thin films fulfill the Raman-Nath conditions. The two-level mechanism of nonlinear absorption in media with the low-saturated absorption is considered. For the first time to calculate an output intensity of any diffracted order of the self-diffracted beams we take into account the effect of interference between two writing beams as well as between their different diffracted orders. We obtain significant gain both in the diffraction efficiency of the self-diffracted beams and in the response time rapidity, that show advantages of using low-saturated absorption media for real-time information processing. The modeling results are compared with experiments provided on dry bacteriorhodopsin thin films and display a good agreement between developed modeling and experiments for a low-saturated absorption medium.

2. Theoretical modeling of Raman-Nath holographic self-diffraction in thin films

We consider time-depended holographic diffraction of laser beams from dynamic phase gratings recorded in thin organic films. We compare diffraction efficiency parameters for a probe beam of weak intensity conventionally used in holographic experiments and for intensive recorded beams.

The scheme of holographic experiment is shown in Fig.1. A beam from He-Ne laser is divided on two beams with equal intensities I_0, which are converged in the thin film under small angel and interfered there. A probe beam of the same wavelength but being not coherent with the recorded beams appeares on the film at the nearly Bragg angle. As the result of beam diffraction from a transmission grating under conditions of thin (Raman-Nath) films, one can observe a number of diffracted orders, but we detect and investigate only the first-order beams. The main feature of beam self-diffraction lies in the fact, that the diffracted orders of each recorded beam are interfered, that leads to significant increasing of their output intensities in comparison with the probe beam diffracted orders.

We start from the wave equation:

$$\Delta E - \frac{\bar{\varepsilon}}{c^2}\frac{\partial^2 E}{\partial t^2} = \frac{1}{c^2}\frac{\partial^2 (\Delta\varepsilon \cdot E)}{\partial t^2} \qquad (1)$$

where the dielectric susceptibility is presented in the form: $\varepsilon = \bar{\varepsilon} + \Delta\varepsilon$. $\bar{\varepsilon}$ is the average dielectric susceptibility of the medium; $\Delta\varepsilon$ is the light induced changes, which assumed to be

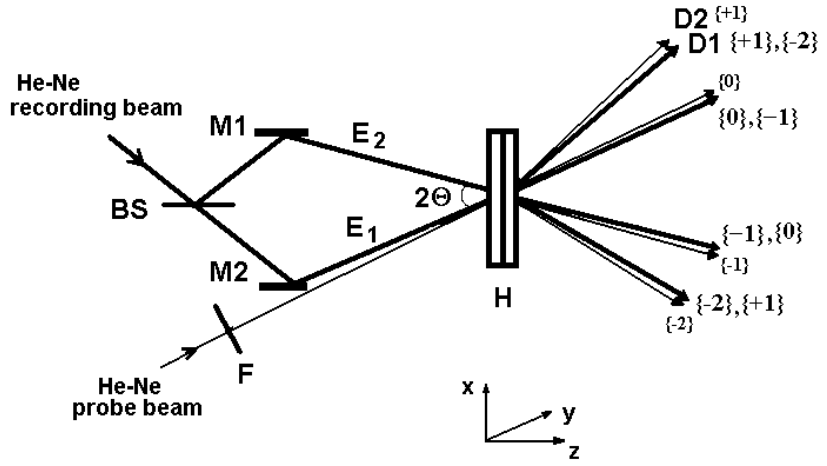

Fig.1. Schematic setup for simultaneous measuring the kinetics of self-diffraction of recording beams and diffraction of an independent probe beam. M1 and M2 are mirrors, BS is a beam splitter, F is a filter, H is a thin film with recorded hologram, E1 and E2 are the recording beams, D1 and D2 are photodetectors. The numbers in figured brackets designate the diffracted order numbers of corresponding beams.

small: $|\Delta\varepsilon| << |\bar{\varepsilon}|$. Let's consider only linear polarized beams, which have the polarization of the electric field directed along the y-axis. We will find the solution of the equation (1) in the form of the Fourier series:

$$E_1^{(y)}(x,z,t) = e^{-i(wt-k_z z)} \times \sum_\ell \overline{R}_\ell(z,t) e^{i\ell k_x x} \quad (2)$$

$$E_2^{(y)}(x,z,t) = e^{-i(wt-k_z z)} \sum_\ell \overline{S}_\ell(z,t) e^{-i\ell k_x x} \quad (3)$$

$$E_{probe}^{(y)}(x,z,t) = e^{-i(wt-k_z z)} \sum_\ell \overline{P}_\ell(z,t) e^{i\ell k_x x} \quad (4)$$

where E_1 and E_2 are the recorded beams; $\overline{R}$, $\overline{S}$ and $\overline{P}$ are the complex amplitudes of the corresponding waves. Every wave-vector $\vec{k}_\ell = k_z\vec{z} \pm \ell k_x \vec{x}$ determines the propagation direction of the ℓ-diffracted order of the beams.

$\Delta\varepsilon$ is spread out on the Fourier series as well:

$$\Delta\varepsilon(x,t) = \sum_m \varepsilon_m(t) e^{imKx} \quad (5)$$

K is the module of the grating vector. As we use the interference light field in the form $I = 2I_0[1+\cos(Kx)]$ to record the dynamic grating, where $\Lambda = 2\pi/K$ is the space period of the interference pattern, the wave-vector and the grating vector are connected by the relation: $|K| = 2k_x$. Applying the presentation (5), we are able to take into account every grating with the grating vectors $K_m = mK$ as well as the wave diffraction from all these gratings. The Fourier components ε_m corresponded to the amplitude of the mK-gratings can be found from the relation:

$$\varepsilon_m = \frac{K}{2\pi} \int_{-\pi/K}^{\pi/K} \Delta\varepsilon(x, I_0, t) \cdot \cos(mKx) dx \quad (6)$$

To solve the wave equation (1) we use the usual approach of slow variable amplitude. We obtain the common equation, which describes the changes of the wave complex amplitude for any ℓ-diffracted order over the distance, in the following form [10]:

$$\frac{\partial \overline{E}_\ell}{\partial \bar{z}} = -i\cos^2\theta(\ell^2 - 1)\overline{E}_\ell + \frac{i}{\bar{\varepsilon}} \sum_{\substack{n,m \\ n\neq m}} \varepsilon_m \overline{E}_{n-m} \exp(ik_x x(m+n-\ell)) \quad (7)$$

where $\bar{z} = z \cdot k^2/(2k_z)$, 2θ is the convergent angle of writing beams, $\overline{E}_\ell$ is used to designate any complex amplitude $\overline{R}_\ell$, $\overline{S}_\ell$ or $\overline{P}_\ell$. The last term on the right side of the equation (7) describes the changes of $\overline{E}_\ell$ wave amplitude due to interference between all diffracted orders during the wave propagation. The index ratio $m+n-\ell = 0$ determines the phase matching condition between different diffracted orders; the waves with the diffracted orders, which satisfy this relation, are added in phase.

We restrict our consideration by the transmission waves, the first- and the second-diffracted orders, which are described by the following indexes (see Fig.1): ℓ=1 for the {0}-order, ℓ=3 for the {+1}-order, ℓ=-1 for the {-1}-order and ℓ=-3 for the {-2}-order. Then the equation (7) will represent the set, which connects 4 differential equations in the case of a probe beam and 8 ones in the case of wave self-diffraction. The sets include three gratings with grating vectors K, 2K and 3K. From these sets all real amplitudes and phases of waves can be obtained.

The output intensity in the direction of the first-order, which we are interested for, in the case of the self-diffraction is determined as the superposition of {+1}-diffracted order of the wave E_1 and {-2}-diffracted order of the wave E_2, that have the same direction of the propagation and are interfered (see Fig.1). This intensity may be defined from the expression:

$$I_3^{self} = |\overline{R}_3 + \overline{S}_{-3}|^2 = R_3^2 + S_{-3}^2 + 2R_3 S_{-3}\cos(\rho_3 - \sigma_{-3}) \quad (8)$$

where R_3, S_{-3} are real amplitudes and ρ_3, σ_{-3} are the phases of the corresponded waves.

In the case of the probe beam we have the only one wave in the direction of the first order

with the intensity:

$$I_3^{probe} = P_3^2 \qquad (9)$$

The presented description may be used to calculate output intensities of any Raman-Nath diffracted orders both in the case of self-diffraction and only for probe beam.

3. Two-level model of nonlinear saturated medium

The main mechanism of holographic grating recording in many light sensitive organic polymers, dyes as well as in bacteriohodopsin films consists in light absorption with consequent transformation of organic molecules, which usually leads to transparency of the films. The simplest model of absorption includes two levels, the non-linear properties lie in the dependence of the absorption value on the intensity of light.

The two-level model shown in Fig.2. N_1 and N_2 are the population densities of the corresponding levels, the total density of absorbed molecules is assumed to be conserved $N_0=N_1+N_2$. The changes of the population density on the level 2 due to light absorption are described by the following balance equation:

$$\frac{dN_2}{dt} = \chi_1 A_1 \frac{I_0}{h\nu} N_1 - \frac{1}{\tau} N_2 \qquad (10)$$

where χ_1 is an absorption cross-section for the level 1, A_1 is a quantum yield of 1⇒2 transition, τ is the lifetime of the level 2.

The equation (10) has the solution of the

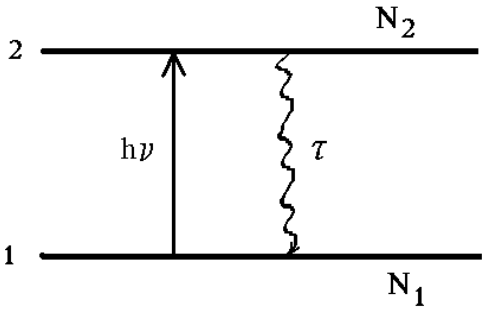

Fig.2. The two-level model of nonlinear absorption.

value N_1/N_0 in the form:

$$\frac{N_1(I,t)}{N_0} = \frac{1}{1+\beta\cdot I} \times \left[1+\beta\cdot I\cdot\exp\left(-\frac{t}{\tau}(1+\beta\cdot I)\right)\right] \qquad (11)$$

The steady state solution is the following:

$$\frac{N_1(I)}{N_0} = \frac{1}{1+\beta\cdot I}, \qquad (12)$$

where $\beta = \frac{\chi_1 A_1}{h\nu}\tau$. The value of β is varied depending on saturation intensity of used materials. For example, a saturation intensity of all types of bacteriorhodopsin films is nearly 10 mW/cm^2 and here β≈4.5 [9].

To record holographic gratings the interference field is applied. The spatial-intensity modulation I(x) in the case of equal input intensities has the form: $I(x) = 2I_0[1+\cos(Kx)]$. Using the Kramers-Kronig relation we can determine the light-induced changes in the refractive index Δn, which is proportional to the relative population density of the level 1: $\Delta n(x,I_0,t) \propto \frac{N_1(x,I_0,t)}{N_0}$. The value Δn obtained due to described mechanism of light absorption (or $\Delta\varepsilon\cong 2n_0\cdot\Delta n$, where n_0 is the average refractive index of a medium) is substituted to the holographic equations, derived in the previous section 2. By this way we obtain the closed modeling, that includes spatial-distributed light-induced absorption in the medium, dynamic grating recording and diffraction of recorded waves (or a probe beam) on the grating.

According to the equations (11) and (12) the modulation strength of the grating will depend on both on the intensity of writing beams and on a time. In Fig.3 we show changes of the grating amplitude profiles both in the kinetics and in the steady state. The upper graphs correspond to the case of weak modulation; the lower graphs correspond to the saturation regime. As shown below the output

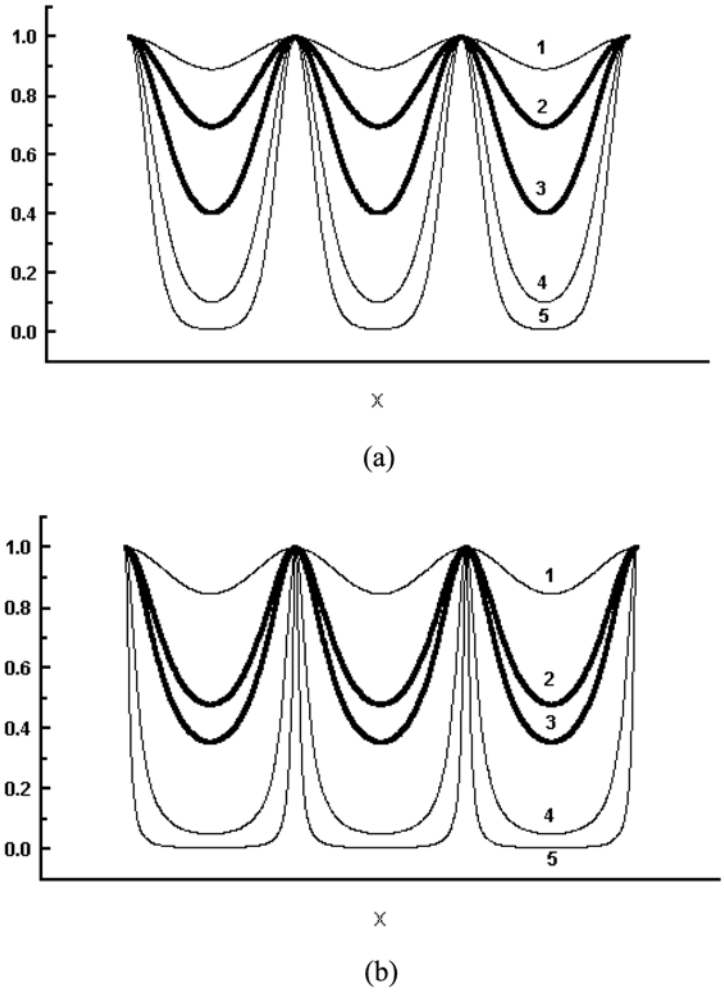

Fig.3. Spatial profile of gratings in a material with low-saturation absorption. (a) The kinetics: I_0=200 a.u., lg(t/τ)=-4.5; -4; -3.6; -3.2; - 2.9 for the curves 1, 2, 3, 4, 5 correspondingly . (b) The steady state: I_0=0.01; 0.06; 0.1; 1; 10 a.u. for the curves 1, 2, 3, 4, 5 correspondingly.

intensities of high-diffracted orders are small for such gratings. At the same time the grating profiles shown in the middle part will give maximum intensities of diffracted beams.

4. Theoretical and experimental holographic kinetics in the case of dry bacteriorhodopsin thin films

We provided the theoretical modeling numerically to calculate intensities of first-order holographic diffraction for both self-diffraction of recorded beams and for a weak probe beam.

The graphs for steady state in dependence with the intensity of the writing beams are shown in Fig.4. One can see the diffraction efficiency that is two times higher in the self-diffraction conditions. Also there is the shift between maximums of the curves. In Fig.3b we depict the grating amplitude profiles, which give these maximums. We obtained two different gratings: the grating 2 for the self-diffracted beams and the grating 3 for the probe beam, which is achieved for higher intensity of the writing beams.

To explain the shift we calculate Fourier coefficients for the dynamic grating in dependence on the input intensity for the steady state. The graphs are shown in Fig.5. One can see the shape of the first-order diffraction efficiency for the probe beam matched with the shape of the first coefficient Fourier ε_1. And the values ε_2, ε_3 determine the diffraction efficiency

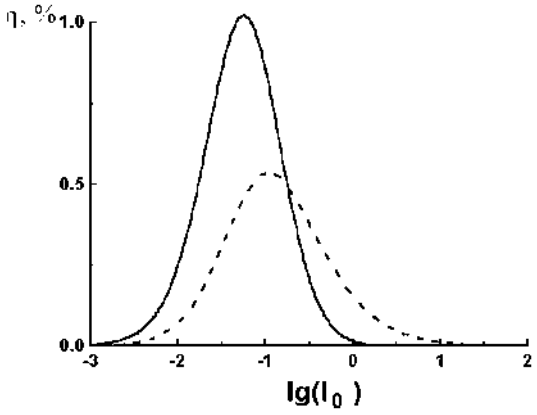

Fig.4. Steady-state diffraction efficiency of the first-order versus of the recording intensity. Solid curve is for the self-diffracted beams, dash curve is for the probe beam.

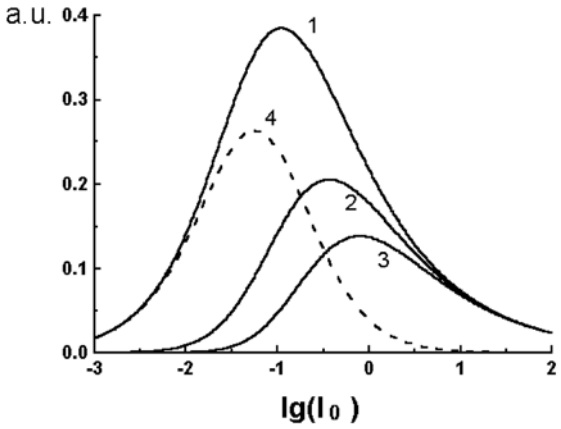

Fig.5. Fourier coefficient values as a function of the recording intensity: ε_1 (the curve 1), ε_2, (the curve 2), ε_3, (the curve 3), $\varepsilon_1+\varepsilon_2$ (the curve 4).

of the probe beam for the second-order and third-order diffraction accordingly. At the same time, the curve 4 is the sum of $\varepsilon_1+\varepsilon_2$. As the even Fourier coefficients are positive and odd ones are negative, the sum maximum is shifted in the area of less intensity in comparison with ε_1. The Fourier coefficient ε_1 determines the {+1}-order of the wave E_1, and the coefficient ε_2 determines the {-2}-order of the wave E_2. The shape of the curve 4 fully agrees with the intensity dependence of the first-order diffraction efficiency of self-diffracted beams (see Fig.4). That proves the fact that first-order output intensity in the self-diffraction condition is the interference of {+1}- and {-2}-orders of both recording beams.

In Fig.6 we calculate the kinetics of the first-order diffracted beams for different intensities of recorded beams. Like in the steady state, the diffraction efficiency of the self-diffraction is more than two times higher in comparison with the probe beam diffraction. We also observed the shift between maximums discussed above. The important results appearing in the fact of obtaining the jump in the diffraction efficiency regardless of the value of the input intensity of recorded beams, that is the peculiar properties of materials with low-saturated

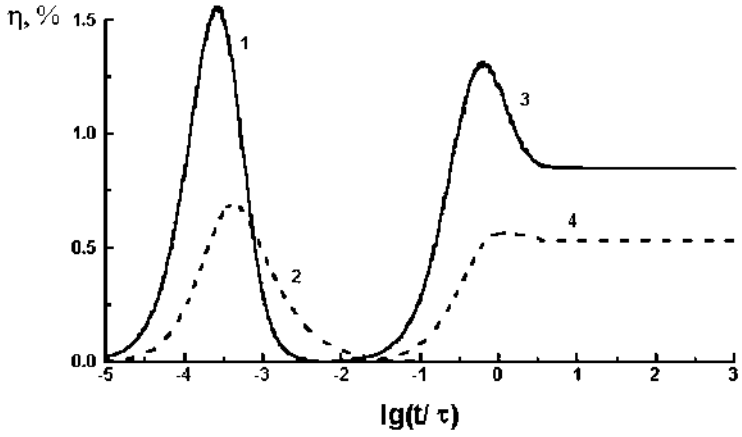

Fig.6. Diffraction efficiency kinetics of the first-order self-diffracted beams (solid curves) and first-order diffracted probe beam (dash curves): I_0=200 a.u.(the curves 1 and 2); I_0=0.1 a.u. (the curves 3 and 4).

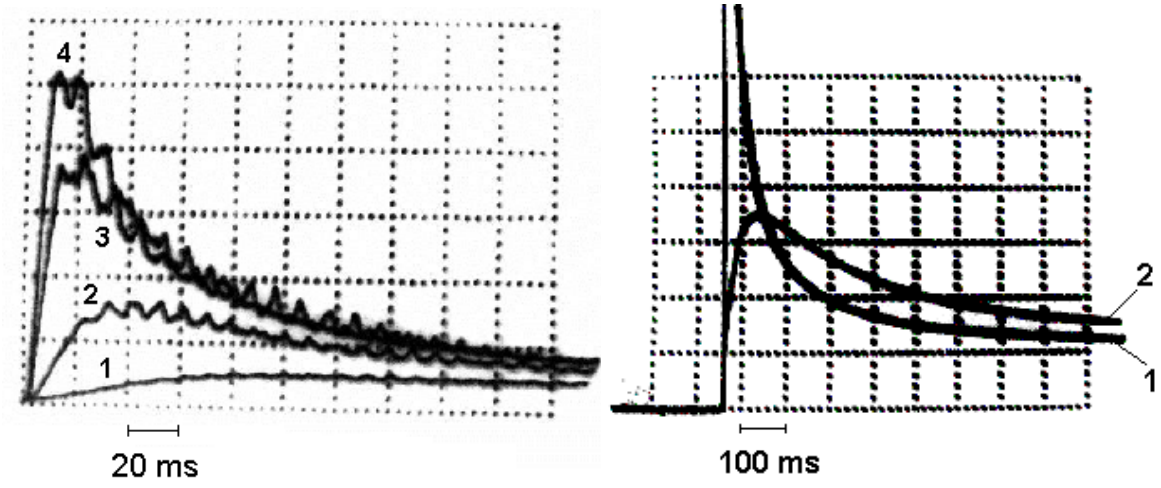

a) b)

Fig.7. Experimental holographic kinetics for dried BR film. (a) Kinetics of the first-order self-diffracted beam at different intensity of the recording beam I_0. 1 – I_0=25 mW/cm^2; 2 – I_0=60 mW/cm^2; 3 – I_0=140 mW/cm^2; 4 – I_0=200 mW/cm^2.(b) Kinetics of the first-order diffracted beams at I_0=200 mW/cm^2. 1 - first-order self-diffraction beams; 2 – first-order diffracted probe beam.

absorption. The jump for high input intensities is rapid and is achieved over a fast period of time. That opens the perspective to employ such materials in novelty filters.

The experimental holographic kinetics for the first-order diffraction are shown in Fig.7 for dry BR films. In Fig.7a there are changes of the output intensities of self-diffracted beams in dependence on input intensities I_0. One can see while increasing I_0, the maximum value of the output intensity is increased as well. The comparative kinetics for the probe beam diffraction and the self-diffraction are shown in Fig.7b. There is a good agreement with the theoretical results shown in Fig.6. In the experiments we observed the significant difference between the diffraction efficiency of the probe beam and the diffraction efficiency of the self-diffracted beams, as well as we observed the shift between their maximums.

By this way our developed theoretical modeling explains the experimental results obtained in BR films. These kinds of modeling can be applied for light sensitive organic thin films that possess the properties of nonlinear low-saturated absorption.

5. Conclusion

Recording dynamic holographic gratings in the saturation region has considerable interest in the area of optical information processing. In this work the numerical model of the holographic grating kinetics of both self-diffraction of recording beams and diffraction of an independent probe beam in the region of saturable absorption is developed. Modeling is performed for a two-level nonlinear absorbed saturated medium. For low-saturated material, the refractive index spatial distribution leads to higher-order diffracted beams. We obtain that interference of higher-order diffracted beams in self-diffraction conditions result in the significantly higher diffraction efficiency in comparison with the diffraction of an independent probe beam on the same grating. Increasing the input intensities of writing beams the rapidity of the response in higher diffracted orders is increased as well, that displays the perspective of using the materials with the low-saturation absorption in real-time information processing, in particular, in novelty filters. The numerical results agree well with experimental ones on the bacteriorhodopsin films.

References

1. Korchemskaya E., Soskin M. Optical Engineering **33**, 3456 (1994).
2. Hampp N. Chemical Reviews **100**, 1755-1776 (2000).
3. Korchemskaya E., Stepanchikov D., Burykin N. Potentials of dynamic holography on bacteriorhodopsin films for real-time optical processing, in Ed. A. Der and L. Keszthelyi, "Bioelectronic Applications of Photochromic Pigments", IOS Press, Amsterdam - Berlin - Oxford - Tokyo - Washington, DC (2001).
4. Rhee Uh-Sock, Caulfield H. John, Vikram Chandra S., Shamir J. Applied Optics **34**(5) (1995), 846-853.
5. Kramer M.A., Tompkin W.R., Boyd R.W.. Physical Review A **34**(3) (1986), 2026-2031.
6. Nikolova L., Todorov T. Opt. Acta **31** (1984), 579.
7. Todorov T., Nikolova L., Tomova N. Applied Optics **23**(24) (1984), 4588-4591.
8. Burykin N., Korchemskaya E. Proc. SPIE **2868** (1996), 196-204.
9. Korchemskaya E., Burykin N., Stepanchikov D. OSA Trends in Optics and Photonics **62** (2001), 370-378.
10. Vinetskii V., Kukhtarev N., Odoulov S., Soskin M. Progress of Phys. Sciences. **129** (1979), 113-137 (in Russian).